



HAL
open science

Brain-spinal cord interaction in long-term motor sequence learning in human: An fMRI study

Ali Khatibi, Shahabeddin Vahdat, Ovidiu Lungu, Jurgen Finsterbusch, Christian Büchel, Julien Cohen-Adad, Veronique Marchand-Pauvert, Julien Doyon

► To cite this version:

Ali Khatibi, Shahabeddin Vahdat, Ovidiu Lungu, Jurgen Finsterbusch, Christian Büchel, et al.. Brain-spinal cord interaction in long-term motor sequence learning in human: An fMRI study. *NeuroImage*, 2022, 253, pp.119111. 10.1016/j.neuroimage.2022.119111 . hal-03744521

HAL Id: hal-03744521

<https://hal.sorbonne-universite.fr/hal-03744521>

Submitted on 3 Aug 2022

HAL is a multi-disciplinary open access archive for the deposit and dissemination of scientific research documents, whether they are published or not. The documents may come from teaching and research institutions in France or abroad, or from public or private research centers.

L'archive ouverte pluridisciplinaire **HAL**, est destinée au dépôt et à la diffusion de documents scientifiques de niveau recherche, publiés ou non, émanant des établissements d'enseignement et de recherche français ou étrangers, des laboratoires publics ou privés.

1
2
3
4
5 Brain-Spinal Cord Interaction in Long-Term Motor Sequence
6 Learning in Human: an fMRI Study
7
8
9

10 Ali Khatibi^{1,2,3,4 †*}, Shahabeddin Vahdat^{1,2,5 †}, Ovidiu Lungu^{1,2,6}, Jurgen Finsterbusch⁷,
11 Christian Büchel⁷, Julien Cohen-Adad^{8,9,10}, Veronique Marchand-Pauvert¹¹, Julien Doyon^{1,2}

12
13 1 McConnell Brain Imaging Center, Montreal Neurological Institute, McGill University, Montreal, QC, Canada

14 2 Centre de recherche de l'Institut Universitaire de Gériatrie de Montréal, Montréal, QC, Canada

15 3 Centre of Precision Rehabilitation for Spinal Pain (CPR Spine), University of Birmingham, UK

16 4 Centre for Human Brain Health, University of Birmingham, UK

17 5 Department of Applied Physiology and Kinesiology, University of Florida, Gainesville, FL, USA

18 6 Department of psychiatry and addictology, University of Montreal, Montreal, QC, Canada

19 7 Department of Systems Neuroscience, University Medical Center Hamburg-Eppendorf, Germany

20 8 NeuroPoly Lab, Institute of Biomedical Engineering, Polytechnique Montreal, Montreal, QC, Canada

21 9 Functional Neuroimaging Unit, CRIUGM, University of Montreal, Montreal, QC, Canada

22 10 Mila - Quebec AI Institute, Montreal, QC, Canada

23 11 Sorbonne Université, INSERM, CNRS, Laboratoire d'Imagerie Biomédicale, LIB, F-75006, Paris, France

24
25 † These authors contributed equally to the work
26
27

28 * Corresponding author:

29 Ali Khatibi, PhD

30 CPR Spine, School of Sport Exercise and Rehabilitation Sciences

31 University of Birmingham, Birmingham, UK

32
33 ali.khatibi@gmail.com
34
35

36 **ABSTRACT**

37

38 The spinal cord is important for sensory guidance and execution of skilled movements. Yet its role in
39 human motor learning is not well understood. Despite evidence revealing an active involvement of spinal
40 circuits in the early phase of motor learning, whether long-term learning engages similar changes in spinal
41 cord activation and functional connectivity remains unknown. Here, we investigated spinal–cerebral
42 functional plasticity associated with learning of a specific sequence of visually-guided joystick
43 movements (sequence task) over six days of training. On the first and last training days, we acquired
44 high-resolution functional images of the brain and cervical cord simultaneously, while participants
45 practiced the sequence or a random task while electromyography was recorded from wrist muscles. After
46 six days of training, the subjects’ motor performance improved in the sequence compared to the control
47 condition. These behavioral changes were associated with decreased co-contractions and increased
48 reciprocal activations between antagonist wrist muscles. Importantly, early learning was characterized by
49 activation in the C8 level, whereas a more rostral activation in the C6-C7 was found during the later
50 learning phase. Motor sequence learning was also supported by increased spinal cord functional
51 connectivity with distinct brain networks, including the motor cortex, superior parietal lobule, and the
52 cerebellum at the early stage, and the angular gyrus and cerebellum at a later stage of learning. Our results
53 suggest that the early vs. late shift in spinal activation from caudal to rostral cervical segments
54 synchronized with distinct brain networks, including parietal and cerebellar regions, is related to
55 progressive changes reflecting the increasing fine control of wrist muscles during motor sequence
56 learning.

57

58

59 **Keywords:** Spinal cord, Brain, Motor Learning, networks, fMRI

60

61

62 INTRODUCTION

63 Over the past decades, a plethora of neuroimaging studies has sought to provide insights into the
64 neurofunctional mechanisms mediating motor learning capacities in humans, given the ubiquity and
65 importance of motor skills in everyday life, and their role during recovery after trauma such as strokes
66 and spinal cord injuries. Motor sequence learning (MSL) is one such skill; it refers to the process during
67 which simple, stereotyped movements come to be performed effortlessly as a unitary sequence through
68 repeated practice. Ample evidence indicates that MSL (a form of procedural memory) takes place over
69 different phases (e.g., fast [minutes to hours] and slow [hours to days]), with different patterns of cerebral
70 neuroplasticity associated with each (e.g., (1-4)). Specifically, changes in neuronal activity in the cortico-
71 cerebellar and cortico-striatal circuits (in conjunction with hippocampus) have been observed from the
72 fast to the slow phase as the motor sequence is being acquired and consolidated (4-7).

73 Yet, an important question, largely overlooked by the neuroimaging community so far, is whether
74 MSL relies on brain plasticity alone, or it involves other parts of the central nervous system (CNS), such
75 as the spinal cord. Traditionally, the spinal cord has been viewed as a mere pathway for relaying signals
76 from higher-order brain regions to the peripheral effectors, and from the sensory cells back to the brain,
77 with a limited role in information processing (8). Yet, a large body of evidence, primarily from animal
78 neurophysiology research using traditional learning paradigms and lesions studies, has revealed that
79 spinal neurons do support habituation and sensitization learning mechanisms, as well as Pavlovian and
80 instrumental conditioning; all representing proxies of spinal cord neuroplasticity (9, 10). Similarly, there
81 is also accumulating evidence from human electrophysiology studies showing that spinal motoneurons
82 excitability (as measured via the Hoffmann H-reflex) can change following a single motor skill training
83 session, hence supporting the hypothesis that intrinsic spinal cord plastic changes can be observed during
84 this form of motor learning (11-15). Indeed, the first direct evidence that MSL relies on neuroplasticity at
85 different levels of the CNS, and that the spinal cord contributes uniquely to this process, has been
86 provided by our group (16). In the latter study, we used an innovative functional magnetic resonance
87 imaging (fMRI) protocol, during which we scanned the brain and cervical spinal cord simultaneously,
88 while participants performed an MSL task (16). This simultaneous brain-spinal cord fMRI protocol
89 allowed us to assess, *in vivo*, the MSL-related activity at multiple CNS levels, and to probe the functional
90 interactions that develop between the spinal and supraspinal levels during motor learning. Importantly,
91 the results from this study, not only revealed an increase in blood oxygenation level dependent (BOLD)
92 spinal cord activity in C6-C8 spinal segments, when comparing the execution of a complex vs. simple
93 sequence of movements, but also for the first time, to demonstrate that this functional change was
94 independent from that of supraspinal sensorimotor structures known to be anatomically connected to the

95 spinal cord or involved in MSL. Finally, our findings also showed that the initially strong functional
96 connectivity between the spinal cord and sensorimotor cortices diminish with learning, while the
97 connectivity between the spinal cord and cerebellum increase over the course of the acquisition process
98 (16). Altogether, our results strongly suggested that during the fast MSL learning phase, the spinal cord
99 contributes distinctively from the brain to the motor learning process.

100 In addition to its role during the early motor skill learning phase, there is evidence that the spinal
101 cord may also contribute to the acquisition of a more proficient motor program, following additional
102 practice during the slow learning phase. Several animal-model studies have indeed provided direct
103 support to this long-term spinal cord plasticity hypothesis (10, 17-19). In humans, indirect evidence of
104 long-term spinal or corticospinal plasticity has also been provided through several neurophysiological
105 studies that revealed a decrease of amplitude in the H-reflex and motor evoked potentials in motor skill
106 experts like athletes and dancers (20-27). Yet, despite these results, there is a lack of conclusive and direct
107 evidence in humans that the spinal cord is involved in the slow learning phase of a new motor skill due
108 primarily to the fact that testing using these electrophysiological paradigms is done offline, and not while
109 subjects are performing the skilled motor behavior of interest. Moreover, unlike fMRI, these
110 electrophysiological techniques do not provide a precise localization of the changes in spinal activity, nor
111 an assessment of these changes and their interaction on a large scale at both spinal and supraspinal levels.

112 To fill this knowledge gap, we thus employed our pioneering simultaneous brain/spinal cord
113 fMRI data acquisition approach (16, 28-30) in young healthy subjects in order to: (1) test the hypothesis
114 that the spinal cord plays an active role in the slow acquisition phase of a novel sequence of movements,
115 and (2) assess changes in the spinal cord – brain functional connectivity occurring during the early and
116 late phases of motor sequence learning.

117

118 **METHODS**

119 **Participants**

120 Thirty young, healthy subjects were recruited to participate in this study. We included only right-handed
121 individuals and excluded those with a history of neurological or psychiatric disease, motor-system
122 complications, use of neurological medication or with any MRI-incompatible object or material in their
123 body. We also excluded individuals who previously participated in motor-learning experiments, as well as
124 those with previous training in playing an instrument for more than three consecutive years in the last five
125 years. Of the participants fulfilling all the inclusion and none of the exclusion criteria, we subsequently
126 excluded the data from two subjects who did not come for the training sessions following the first day of

127 scanning, and from another subject who had excessive movements (more than 7mm in plane) during the
128 neuroimaging session while executing the motor task, hence resulting in failed motion correction. Thus,
129 the final sample considered for analysis consisted of 27 participants (14 females, mean±SD age = 24.85 ±
130 2.98 years old). The ethics committee at the Centre de Recherche de l'Institut Universitaire de gériatrie de
131 Montréal (CRIUGM) reviewed and approved the study (protocol number: CMER-RNQ 15-16-06). All
132 participants gave written informed consent at the beginning of the experiment and were debriefed and
133 compensated for their participation after having completed the experiment.

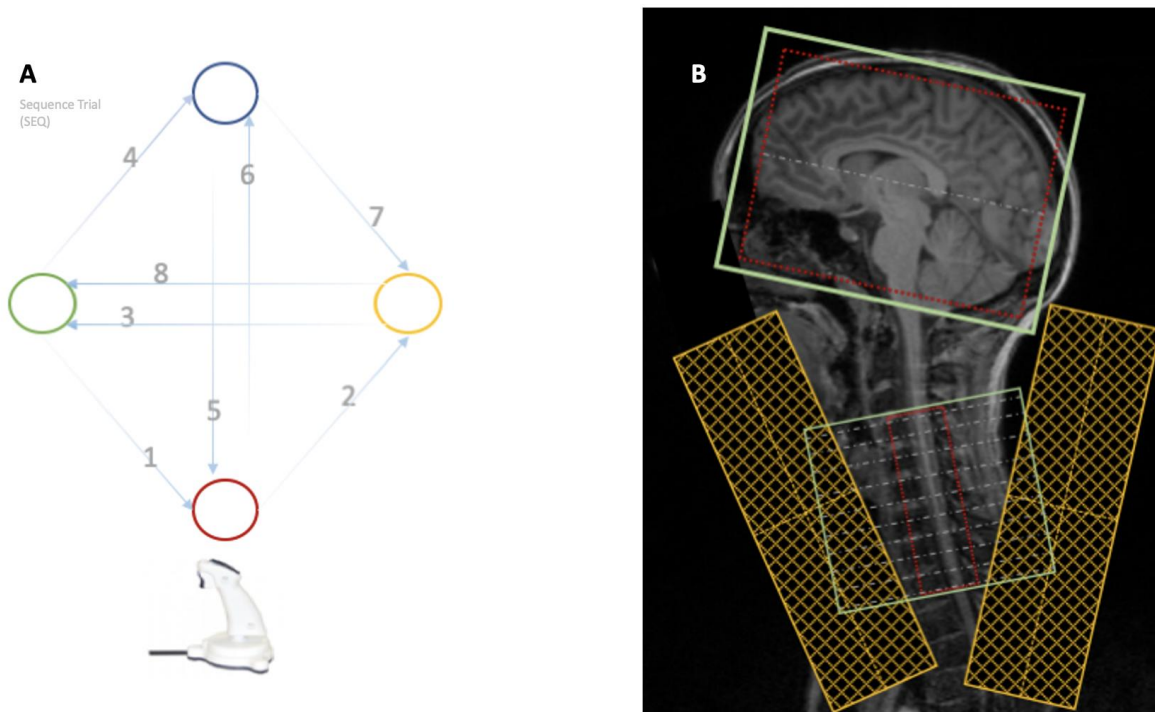
134 **General procedure**

135 The study consisted of 6 testing sessions, which occurred daily over a period of 6 days. Participants were
136 scanned twice; at the beginning and at the end of a 6-days motor skill learning regimen. On Day 1,
137 participants were acquainted with the set-up by practicing the MSL task inside a mock MRI scanner. The
138 sequence of movements practiced in the mock scanner was different from the other sequence used during
139 the actual experiment. Following the participant's habituation with the experimental set-up and task, they
140 were then moved into the actual 3.0T MRI scanner, where they were asked to perform both the sequence
141 and random conditions of the motor task (please, see the task description below for more details). For the
142 next four behavioral-only sessions, each taking place on subsequent days, participants were placed inside
143 the mock MRI scanner and asked to perform the sequence learning condition (SEQ, see below). Finally,
144 on Day 6, subjects were again tested (at the same time of the day as the Day 1) and scanned following the
145 same procedures as the one used in the first session, except for the habituation period.

146 **Motor sequence learning paradigm**

147 Participants performed the motor task using a joystick manipulated by their dominant (right) hand (Fig. 1-
148 A). The task began with the visualization of a cursor (i.e., a black circle) in the center of the screen, which
149 showed the location of the joystick corresponding to the neutral position of both the joystick and the
150 wrist, and of 4 static targets located clockwise at 3, 6, 9 and 12 o'clock, corresponding to wrist abduction,
151 flexion, adduction and extension, respectively. Participants were instructed to move the cursor to the
152 location of a target as soon as the circle was filled (by moving the joystick toward the corresponding
153 location). As soon as the cursor touched the target's location, the latter disappeared, and the next target
154 appeared at another location among the 3 remaining targets. Participants were asked to reach targets as
155 quickly as possible, but unbeknown to them, a repeating sequence of 8 locations was repeated ten times in
156 a block of 80 trials. There was a short break (20 seconds) between two consecutive blocks and each
157 session comprised a total of 15 blocks. Two different conditions of the motor task were administered. In
158 one condition, the targets appeared in a sequential order that was repeated every 8 trials (8-item sequence
159 learning condition; SEQ), whereas in the other condition, the targets appeared in a pseudorandom non-

160 sequential order (random condition; RND). The specific sequence (Fig. 1A) was selected such that each
161 target was hit twice, and no transition was repeated twice. We also made sure that, on average, the
162 random condition followed the same distribution of targets and transitions. Same number of blocks and
163 trials used in each session. Overall, the average time of the participants to complete the motor sequence
164 training on day 1 was around 30 minutes while it reduced to less than 25 minutes after 6 days of practice.
165



166
167 **Figure 1.** (A) Illustration of the sequence of movements that subjects were required to practice during
168 each session. Subjects were asked to perform the task using an MRI compatible joystick that they
169 manipulated with their (dominant) right hand. (B) The shimming and scanning parameters were adjusted
170 for each sub-volume (brain, spinal cord) separately described in (29). The brain sub-volume covered the
171 whole cerebrum (30-33 slices), while the spinal cord sub-volume covered the C3-T1 segments of the
172 spinal cord (8-10 slices).
173

174 MRI Data Acquisition

175 To investigate reciprocal influences of the brain and the spinal cord during motor learning, we used a
176 specific MRI pulse sequence that enabled us to acquire BOLD data simultaneously from the cervical
177 spinal cord and brain (29, 31). Specifically, this sequence allowed us to acquire data from 2 sub-volumes
178 of images within the same TR, one covering the cervical spinal cord (C3-T1 spinal segments), and one
179 covering the entire brain, with different field of view and spatial resolutions (Fig. 1-B). At the beginning
180 of the scan session, five sample echo-planar imaging (EPI) volumes were acquired, and the acquisition

181 parameters for each of these 2 sub-volumes were optimized to ensure optimal quality data for both the
182 brain and cervical spinal cord. For this purpose, shimming properties and resonance frequencies were
183 adjusted individually for each of the 2 sub-volumes prior to the start of the test runs in each scanning
184 session and were then updated during BOLD signal recording in the brain and the spinal cord. Details of
185 this shimming procedure are discussed elsewhere (31). In addition and based on those pre-scan
186 acquisitions, a specific "z-shim" slice-specific approach was used to maximize the signal intensity within
187 the cervical spinal cord (32). Due to the size of the area, and to reduce the likelihood of displacement and
188 artifacts related to magnetic susceptibility differences between bone and soft tissue, a small rectangular
189 shim box (red box, Fig. 1B) was placed around the cord.

190 A 3T TIM Trio Siemens MR scanner (Siemens Healthcare, Erlangen, Germany) equipped with a
191 12-channel head coil paired with a 4-channel neck coil (both receive only) was used for the current study.
192 Participant's head and neck were supported with extra foam pads to minimize movements during
193 scanning. The lower edge of the head coil (along with the upper lip of the participant, approximately C2-
194 C3 vertebrae) were aligned to the magnet isocenter for optimal coverage.

195 For functional imaging, a total number of 40-43 EPI slices (depending on the participant's head
196 size) were acquired in descending-order for both sub-volumes (interleaved within each volume). The
197 upper sub-volume covering the brain contained 30-33 transversal slices. The whole brain of most
198 participants fitted within this volume, except for a few subjects for whom the box was tilted upward
199 approximately 10 degrees (around the X-axis), thus cutting a small part of the upper motor cortex,
200 specifically the part that corresponds to the lower limbs, which were not involved in the current task.
201 Slices in the brain sub-volume had a field of view (FoV) of $220 \times 220 \text{ mm}^2$, with $2 \times 2 \times 3.5 \text{ mm}^3$ voxel size
202 and a 3.5 mm gap between slices. The flip angle was 90° , the bandwidth per pixel was 1515 Hz yielding
203 an echo spacing 0.74 ms. We used a 7/8 partial Fourier encoding and parallel imaging (GRAPPA) with an
204 acceleration factor of $R=2$ and 48 reference lines to minimize the echo time, hence resulting in an echo
205 train length of 35.6 ms and an echo time of 30 ms for the brain. Parallel imaging also helped reducing
206 image distortions.

207 The lower sub-volume included 8-10 slices covering the cervical spinal cord from C3 to T1 spinal
208 segmental levels and was oriented parallel to the spinal cord at the C6 level. Slices in the lower sub-
209 volume had an FoV of $132 \times 132 \text{ mm}^2$, with $1.2 \times 1.2 \times 5 \text{ mm}^3$ voxel size and 9 mm gap between slices. The
210 flip angle was 90° , the bandwidth per pixel was 1263 Hz yielding an echo spacing of 0.90 ms. 7/8 partial
211 Fourier and parallel imaging ($R = 2$, 48 reference lines) was again used, resulting in an echo train length
212 of 43.3 ms and an echo time of 33 ms. Finally, the TR for the measurement of all slices (brain + spinal
213 cord) was 3140 ms, except for 3 subjects who had a TR of 3050 ms or 3200 ms (depending on each

214 participant coverage within the field of view). Both brain and spinal cord sequences included a fat
215 saturation pulse.

216 Furthermore, two saturation pulses were applied in a V-shaped configuration to minimise
217 ghosting and inflow artifacts related to blood flow in the major cervical vessels. To reduce the level of
218 noise during the functional acquisition runs, signal from the head coil was only used for the brain images,
219 while signal from the neck coil was only used for the spinal cord images, using specific reconstruction
220 procedure described elsewhere (29). The average (\pm SD) temporal signal to noise ratio (tSNR) within the
221 brain and spinal cord masks were 48.1 ± 13.3 and 12.5 ± 4.1 respectively.

222 For structural scanning, we employed two imaging sequences. First, we used a 3D-MPRAGE T1-
223 weighted sequence with the following characteristics: 175 sagittal slices covering entire head and neck
224 down to the C8/T1 vertebrae, TR = 2.3 s, TE = 3.45 ms, FA = 9°, TI = 1.1 s, FoV = 192*240*320, with a
225 voxel resolution of $1*1*1$ mm³. In addition, we used a T2-weighted MEDIC sequence with the following
226 parameters: 12 transversal slices, slice thickness = 5 mm (no gap), in-plane resolution = $0.6*0.6$ mm², TR
227 = 464 ms, TE = 22 ms, FA = 20°, bandwidth 180 Hz per pixel, FoV = 184*256 mm², GRAPPA
228 acceleration factor = 2, reference lines = 48. The latter slices were placed at the same position to the ones
229 used for the spinal fMRI sequence. The T2 image enabled us to acquire a proper GM/WM contrast in the
230 spinal cord and to improve our segmentation and registration outcomes. We also recorded the
231 participants' heart rate (using pulse oximeter) and breathing rhythms during each, the latter measures
232 being used for physiological noise modeling for the spinal cord fMRI data analyses using the
233 Physiological Noise Modelling (PNM) toolbox from the FSL platform (see supplementary information
234 for more details).

235 **Scanning Procedure**

236 After moving to the real scanner and following the localizer and the initial shim process, the first of the 2
237 structural volumes (T1) was acquired, followed by 2 runs of fMRI data. The order of the 2 runs (RND or
238 SEQ conditions) was counterbalanced between subjects. Subjects were not informed explicitly about the
239 experimental conditions to prevent possible expectation bias interference. The functional runs were then
240 followed by the second structural imaging (T2s) scan. The procedure used for the second scanning session
241 (Day 6) was the same as the one employed in the first scan session, except that there was no additional
242 practice of the motor sequence inside the mock-scanner.

243 **MRI data processing**

244 Image processing was done separately for the brain and the cervical spinal cord using the spinal cord
245 toolbox (SCT-v3.1; (33)), FSL-6.0 (34)) and in-house Matlab-2016a programs. Details about Image

246 processing and the analysis of MRI data is provided in supplementary information. Briefly, spinal cord
247 fMRI processing was started with the removal of the first two volumes, and then motion correction was
248 done. The spinal cord was segmented in the motion-corrected images and then registered to the MNI-
249 Poly-AMU template by first registering the image to T2 and then back to the template. After smoothing
250 and high-pass filter, the data was used along with Physiological Noise Modelling (PNM) regressor for the
251 analysis. Brain fMRI data was started with the removal of the first two volumes, then slice timing
252 correction and motion correction. Motion-corrected images were registered to the MNI-152 template
253 using the high resolution T1 images. High-pass filter and smoothing were done before the analysis.

254 **EMG Recording and Preprocessing**

255 EMG signals were recorded using MRI compatible surface electrodes from two muscles, flexor carpi
256 radialis (FCR) and extensor carpi radialis (ECR), while subjects were in the scanner performing the task.
257 EMG was recorded using a Biopac EMG100C-MRI smart amplifier with the sampling rate equal to 2500
258 Hz (gain = 500). Online noise filtering was done using 2 analogue filters for the FCR and ECR muscle
259 activity (Fig. S1A). Offline preprocessing of the EMG signal and automatic artifact removal (AAR) were
260 carried out by estimating the periodicity of MRI gradient artifacts on the raw EMG time series, and then
261 using a sliding average template of these artifacts to subtract them from the signal during each run.

262 The raw time series were first up-sampled ten times, from 2.5 to 25 kHz, to facilitate the temporal
263 interpolation of the signal. To compensate for temporal drift of the artifact over time, we then detected the
264 local maximum for each TR, and computed the peak intensity in the time series that corresponded to the
265 slice excitation. We performed a temporal interpolation of the signal such that the number of data points
266 between 2 peaks were constant and equal to the real TR. Once the time series had the exact same number
267 of points for each TR, we were then able to compute an artifact template. To account for the small
268 fluctuations in MRI artifacts over time, we used a sliding average of 21 TRs to compute local templates
269 instead of calculating a global template of the artifact and subtracted these from the signal. Finally, we
270 down-sampled the resulting time series from 25 kHz back to its original sampling frequency (i.e., 2.5
271 kHz). Figure S1 presents snapshots of the raw EMG signal, as well as of cleaned (denoised) signal.

272 **Performance and EMG Analysis**

273 In order to use the rich kinematics/trajectory data recorded from joystick and assess learning-related
274 changes in movement kinematics, we used a measure of jerkiness instead of simply calculating the
275 reaction times for hitting targets (35). To assess the participants' performance in each block, a measure of
276 jerkiness of movement for reaching the next target was calculated from the third time derivative of pointer
277 displacement (or the second derivative of velocity). The absolute value of the jerk at each time point was
278 calculated and then integrated over time throughout the task to calculate the integrated absolute jerk (IAJ)

279 (36). The mean IAJ scores in the first 7 blocks and the last 7 blocks were calculated separately to assess
280 learning within the run of 15 blocks, with the hypothesis that the movements will become smoother in the
281 SEQ condition as a result of learning.

282 For the EMG data preprocessing, full-wave rectification was applied on the AAR-cleaned EMG
283 signal, followed by low-pass filtering (Butterworth filter, $f_{co} = 10$ Hz) to obtain a measure corresponding
284 to the envelope of EMG signal. For each muscle and condition, the envelope signal was then divided by a
285 normalization factor to account for EMG electrode placement differences across days. This factor was
286 obtained by taking the median value of the root mean square (RMS) of the EMG in a 500-ms sliding
287 window during RND blocks in each session, given that the movement velocity in the RND condition was
288 not different across sessions. We then calculated measures of the “wasted”, “effective” and “total” signals
289 between the pair of antagonistic muscles (FCR and ECR) using their normalized envelope EMG signal at
290 each time point t , as follows (37):

291 Equation 1.

$$\begin{aligned} 292 \quad & \text{total}(t) = \text{FCR}(t) + \text{ECR}(t) \\ 293 \quad & \text{effective}(t) = |\text{FCR}(t) - \text{ECR}(t)| \\ 294 \quad & \text{wasted}(t) = \min[\text{FCR}(t), \text{ECR}(t)] \end{aligned}$$

295 We then estimated the level of co-contraction between FCR and ECR (37) and their reciprocal
296 activity (38), as follows:

297 Equation 2.

$$\begin{aligned} 298 \quad & \text{Co-contraction} = 2 * \text{RMS}[\text{wasted}(t)] / \text{RMS}[\text{total}(t)] \\ 299 \quad & \text{Reciprocal activation} = \text{RMS}[\text{effective}(t)] / \text{RMS}[\text{total}(t)] \end{aligned}$$

300 where RMS is the root mean square operator calculated during each movement element. Then, for each
301 condition and session, the co-contraction and reciprocal activation values were averaged across 4
302 movement elements along the direction of wrist flexion/extension, where the FCR and ECR muscles
303 mainly act as antagonists.

304 Furthermore, as EMG activity, and hence EMG power, is closely related to movement speed (39),
305 EMG signals were additionally normalized using the mean movement speed in each movement block in
306 order to account for differences in speed across blocks and conditions. Hence, we measured the EMG
307 power in each trial by calculating the RMS of the normalized envelope signal during each individual
308 movement element (from one target to the next one). For each muscle and condition, the EMG power was
309 then averaged across all movement elements in that condition. The average EMG power between FCR
310 and ECR muscles were also calculated. Note that normalization through the use of the movement speed
311 does not affect the calculation of co-contraction and reciprocal activation, as the speed normalization

312 factor would be cancelled out in the numerator and denominator, as indicated by the formulas in Equation
313 2.

314 **Statistical Analysis**

315 For the purpose of presentation, the mean \pm standard error of the mean (SEM) is reported. A repeated
316 measure ANOVA with Blocks (1:7 vs 9:15) * Day (Day 1 vs. Day 6) * Conditions (SEQ vs. RND) as the
317 within-subject factors was run on the mean IAJ. Paired sample t-tests were used to compare the first seven
318 blocks with the last 7 blocks of each run within each session. Normality and equality of variance were
319 checked for each analysis and the degree of freedom was adjusted when needed. Alpha level was set to
320 0.05 for all analyses.

321 **RESULTS**

322 **Behavioral Results**

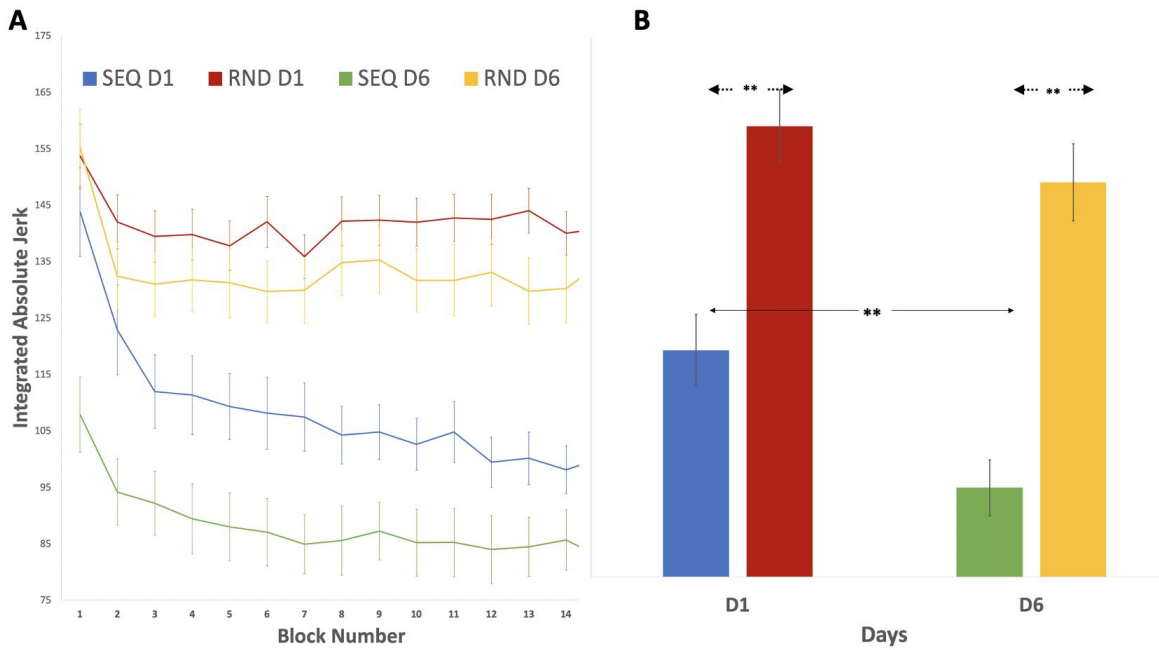
323 Figure 2A displays the block-by-block changes in performance (mean IAJ) for all participants as well as
324 for both conditions (SEQ vs. RND) and days (1 vs. 6) of training, while Figure 2B presents the mean IAJ
325 for each condition across 2 two days of practice.

326 A significant main effect of block [$F(1,26) = 28.03$; $p < 0.001$; $\eta^2_p = 0.52$], day [$F(1,26) = 4.61$; p
327 < 0.04 ; $\eta^2_p = 0.15$], and condition [$F(1,26) = 208.82$; $p < 0.001$; $\eta^2_p = 0.89$], as well as a significant
328 three-way interaction between block, day and condition [$F(1,26) = 8.01$; $p = 0.009$; $\eta^2_p = 0.24$]. When
329 decomposing the 3-way interaction, we noticed that it could be explained by the following two-way
330 interactions: that is between block and condition [$F(1,26) = 25.66$; $p < 0.001$; $\eta^2_p = 0.50$], and between
331 day and condition [$F(1,26) = 10.39$; $p = 0.003$; $\eta^2_p = 0.75$], indicating that the learning effect
332 (operationalized as significant performance changes in the Sequence, but not in the Random condition)
333 was evident within and between each practice day.

334 Paired sample t-tests comparing the first and the last 7 blocks of each day and condition (see Fig.
335 S2) showed that subjects' trajectories for reaching a target were significantly less jerky in the last 7, as
336 compared to the first 7 blocks of practice on each day during the SEQ condition [SEQ-D1: $t(26) = 4.63$, p
337 < 0.001 ; SEQ-D7: $t(26) = 4.67$, $p < 0.001$], whereas there was no such significant difference in the RND
338 condition [RND-D1: $t(26) = -0.23$, $p = 0.82$; RND-D7: $t(26) = 1.52$, $p = 0.14$]. This indicates that
339 learning-related changes (i.e., reducing jerkiness with practice) were evident in the SEQ condition in each
340 training session, where participants could make use of the sequential pattern to perform smoother
341 movements, but not in the RND condition when stimuli appeared at unpredictable locations. This
342 interpretation is further supported by the fact that, on Day 1, participants' trajectories for reaching a target
343 in the SEQ condition were significantly less jerky than those in the RND condition [$t(26) = 9.49$, $p <$

344 0.001]. Similarly, the trajectories for reaching a target in the SEQ condition on Day 6 were also
 345 significantly smoother than those in the RND task [$t(26) = 14.85, p < 0.001$]. In addition, there was a
 346 significant improvement in jerkiness (a reduction in mean IAJ) when comparing the subjects' trajectories
 347 in the SEQ condition across days (less jerky on Day 6 than Day 1) [$t(26) = 3.25, p = 0.003$], whereas there
 348 was no such difference between days in the RND condition [$t(26) = 1.10, p = 0.28$].

349



350

351 **Figure 2.** (A) Block by block subjects' performance across days and conditions, (B) Comparison of the
 352 subjects' performance in the Sequence (SEQ) versus Random (RND) conditions on both Day 1 and 6. Y-
 353 axis represents the Mean Integrated Absolute Jerk (IAJ) index for all movements in a block. Error bars
 354 represent standard error of the mean. * $p < 0.05$; ** $p < 0.01$.

355 **Neuroimaging Results**

356 We had 2 main goals in the current study: first, to examine spinal cord's involvement in motor sequence
 357 learning and second, to characterize the changes in functional connectivity between the brain and spinal
 358 cord associated with the short vs. long-term phases of motor learning.

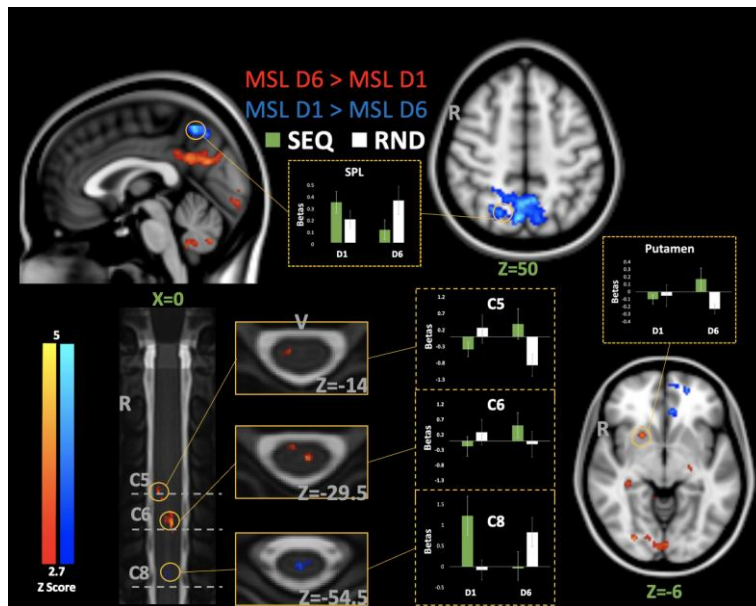
359 Neural Correlates of Short-term and Long-term Motor Sequence Learning: Within Session Effects.

360 As expected, an analysis contrasting the results of the SEQ vs. RND conditions on Day 1, hence reflecting
 361 within-session short term MSL functional changes (Fig. S8A), yielded clusters of activation in the C8
 362 segment of the spinal cord. The peak was located ipsilateral to the hand used in the motor sequence
 363 learning task. Results of the same contrast at the brain revealed clusters bilaterally in the anterior insula
 364 and the SMA, as well as the right anterior cingulate cortex (ACC) and lobule V of the right cerebellum
 365 (Table S5-A).

366 The same contrast assessing the within-session changes specific to long-term MSL on Day 6
 367 (Figure S8-B) revealed 3 clusters of increased activity more rostrally than the one found on Day 1, that is
 368 between C6-C8 segments of the spinal cord, with peaks located both ipsilateral and contralateral to the
 369 hand used for the task. The same contrast at the brain level, yielded activation bilaterally in the anterior
 370 cingulate cortex, the right cerebellum lobule IV, and the left cerebellar lobule V (Table S5-B). This
 371 pattern of results suggests a switch of activity from more caudal regions of the spinal cord on Day 1 to
 372 more rostral regions of the spinal cord on Day 6 of learning. At the cerebral level, the Day 1 to Day 6
 373 transition resulted in more activity in cerebellar regions such as ACC and cerebellum and less activity in
 374 superior parietal lobule (SPL) and Insula.

375 Neural Correlates of Short-term and Long-term Motor Sequence Learning: Between session effects.

376 Comparing the results of the short vs. long-term MSL (SEQ > RND and Day 1 > Day 6; Fig. 3: blue), the
 377 analysis yielded an activation cluster in the spinal cord at the level of the C8 segment with the peak on the
 378 right (ipsilateral) side. The same contrast at the brain level resulted in activations in the superior parietal
 379 lobule bilaterally (peak on the left), the anterior cingulate cortex, the right superior parietal lobule, and the
 380 right lateral occipital cortex (Table S6-A).



381
 382 **Figure 3.** Neural correlates of short-term (Sequence (SEQ) > Random (RND) and Day 1 > Day 6: blue)
 383 vs. long-term (SEQ > RND and Day 6 > Day 1: red) motor learning. MSL represents the contrast between
 384 SEQ and RND conditions. Bar graphs (green = SEQ, white = RND) show the change in beta values
 385 across days and conditions. Coordinates in the brain are based on the MNI-152 template. All activation
 386 maps are corrected for multiple comparisons using Gaussian Random Field (GRF), $p < 0.01$. Coordinates
 387 in the spinal cord are derived from the MNI-Poly-AMU template. Error bars represent standard error of
 388 the mean. SPL = Superior Parietal Lobule.

389 The reverse comparison (SEQ > RND, Day 6 > Day 1; Fig. 3: red) in the spinal cord resulted in 2
390 activation clusters: one in the C5 and on the right ventral side and one in C6 in the center with the peak on
391 the left side on the cord. The same contrast applied at the brain level produced activation clusters in the
392 right putamen, the right posterior cingulate, the right occipital pole, and the right cerebellum lobule IX
393 and vermis lobule VIII.

394 Neural Correlates of Long-term Sequence Practice

395 We contrasted the activation across days (Day 6 vs. Day 1) for the SEQ condition only (SEQ D6 > SEQ
396 D1; Fig. S9: Red-Yellow) to examine the neural correlates of sequence practice only. This analysis
397 resulted in clusters of activity in the right posterior cingulate and cuneal cortices, as well as in the inferior
398 part of the right superior parietal lobule. The same contrast in the spinal cord yielded activation in the
399 rostral part of the C7 segment (on the left side, dorsally). The reverse contrast for the SEQ condition
400 (SEQ D1 > SEQ D6; Fig. S9: Blue-Light Blue) resulted in significant activation clusters in the right
401 superior parietal lobule, the globus pallidus, and the right inferior temporal gyrus at the brain level,
402 whereas it yielded activation in the rostral part of the C8 segment of the spinal cord (on the right side and
403 ventrally). In line with the findings of earlier analyses, here we also noticed changes in the activation foci
404 within the spinal cord from the caudal to more rostral segments as the motor sequence was practiced over
405 many days.

406

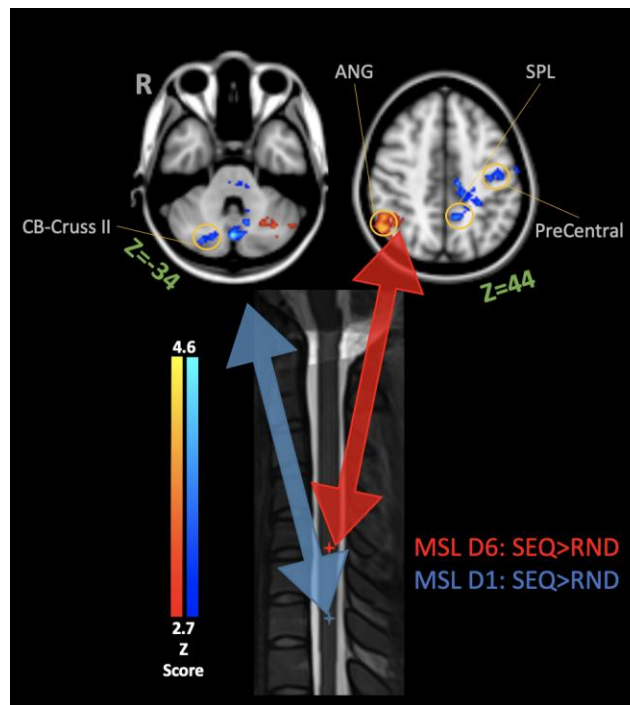
407 We computed correlations between behavioral learning-related changes in motor learning (i.e.,
408 reduction in jerkiness of the movement) and activation values in the brain and spinal clusters in order to
409 provide further evidence that these functional neurophysiological changes are related to motor learning.
410 To this end, we calculated the correlation of the between-session difference in mean jerkiness with the
411 beta values extracted from the clusters of activation in the brain and spinal cord, resulting from the
412 contrast between the sequence practice on Day 1 and Day 6 (figure S9). In the brain, there was a positive
413 correlation between the beta values extracted from SPL and the improvement in performance on the
414 sequence task on Day 1 ($P(27)=0.73$, $p<0.001$). By contrast, in the spinal cord, there was a single positive
415 correlation between the beta values extracted from the cluster surviving the Day6>Day1 contrast and the
416 improvement in performance for the sequence condition on Day 6 ($P(27) = 0.81$, $p < 0.001$).

417 Learning Dependent Interaction Between the Spinal Cord and the Brain

418 Furthermore, we investigated the changes in functional interaction between the local spinal network that
419 was activated during the course of learning and the cerebral network involved in motor sequence learning
420 using PPI analysis (see the description in methods). Here we report the results of the PPI analysis for the
421 learning effect (SEQ>RND) on Day 1 and Day 6 separately. Our results revealed that on Day 1, activity

422 found in the C8 segment of the spinal cord was correlated with that of the left precentral gyrus, the left
423 superior parietal lobule, the brainstem, and right cerebellum (crus I and crus II) in the SEQ compared to
424 the RND condition (Fig. 4, yellow-red; GRF corrected, $p < 0.01$). Furthermore, spinal cord activity on
425 Day 6 (levels C6-7) was correlated with that of the right angular gyrus and left cerebellum (crus I) in the
426 SEQ compared to the RND condition (Fig. 4, blue-light blue; GRF corrected, $p < 0.01$).

427



428

429 **Figure 4.** Activation maps showing brain regions for which their functional connectivity with the spinal
430 cord seeds [Region of interest: (SEQ>RND) Day 1, blue cross and (SEQ>RND) Day 6, red cross] was
431 higher during the Sequence (SEQ) than during the Random (RND) condition. The blue cluster presents
432 positive activation in Day 1, and red clusters present significant activation in Day 6 ($p < 0.01$, corrected
433 for multiple comparisons using GRF). ANG=Angular Gyrus, CB=Cerebellum, SPL=Superior Parietal
434 Lobule

435

436

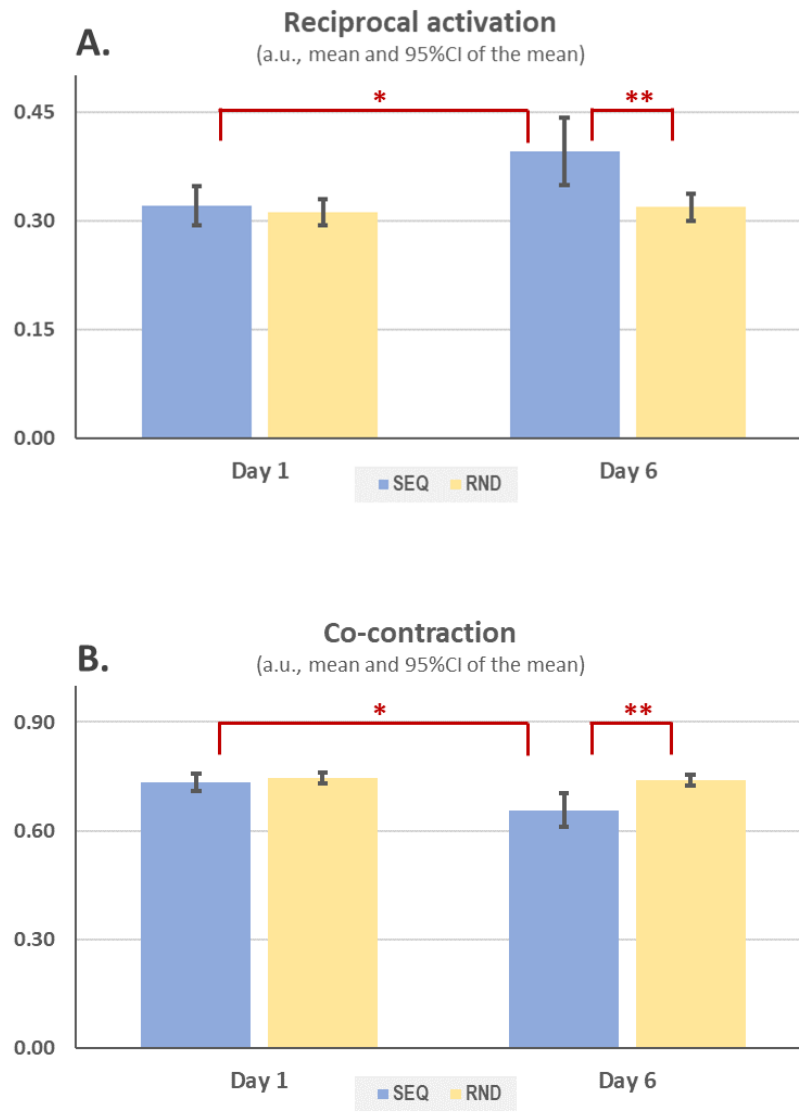
437 **Learning-related Changes in EMG Activity**

438 As changes in the spinal cord activation might be closely related to/manifested by EMG activity, we
439 computed 3 different scores to assess changes in FCR and ECR muscle activities (the main muscles
440 involved in the task) as a result of motor learning. First, we calculated the strength of reciprocal activation
441 between FCR and ECR muscle pair during flexion and extension movements, that is when they act as
442 antagonistic muscles (see Equation 2, Methods). This measure of reciprocal activation was differently
443 modulated in the SEQ and RND conditions depending on the practice day (significant interaction, day

444 (Day 1, Day 6) by condition (SEQ, RND) repeated measures ANOVA, $F(1,26) = 5.99, p = 0.02$ (Fig.
445 5A). Pairwise comparisons revealed higher reciprocal activation in the SEQ condition compared to RND
446 condition on Day 6 ($t(1,26) = 3.5, p = 0.002$), as well as in the SEQ condition on Day 6 compared to Day 1
447 ($t(1,26) = 2.47, p = 0.02$). By contrast, the strength of reciprocal activation did not differ between the SEQ
448 and RND conditions on Day 1 ($p > 0.4$), nor between the RND conditions on Day 1 and Day 6 ($p > 0.5$).

449 Next, we calculated the measure of co-contraction of FCR and ECR muscle pair during flexion
450 and extension movements (see Equation 2, Methods). As for the measure of reciprocal activation, the
451 amount of co-contraction was also differently modulated in the SEQ and RND conditions depending on
452 the practice day (significant interaction, day (Day 1, Day 6) by condition (SEQ, RND) repeated measures
453 ANOVA, $F(1,26) = 6.75, p = 0.01$) (Fig. 5B). Pairwise comparisons further revealed decreased levels of
454 co-contraction in the SEQ condition compared to RND condition on Day 6 ($t(1,26) = 3.76, p < 0.001$), as
455 well as in the SEQ condition on Day 6 compared to Day 1 ($t(1,26) = 2.6, p = 0.01$). Again however, the
456 level of co-contraction between the SEQ and RND conditions on Day 1 ($p > 0.2$), or between RND
457 conditions on Day 1 and Day 6 ($p > 0.5$) did not differ.

458 Finally, we calculated the average EMG signal power of FCR and ECR muscles during task
459 performance (see Equation 2, Methods). For this analysis, EMG was further normalized by movement
460 speed to account for differences in speed across days and conditions (see methods). A two-way repeated
461 measures ANOVA with the normalized EMG power as dependent variable showed no significant
462 interaction between Day and Condition ($p > 0.6$) (Fig. S10). Also, the normalized EMG power did not
463 differ between Day 1 and Day 6 (no main effect of Day, $p > 0.9$), or between SEQ and RND conditions
464 (no main effect of Condition, $p > 0.2$). Overall, our EMG analyses showed that long-term motor learning
465 through multiple days of practice changes the activation pattern in antagonistic muscles, while the
466 average EMG power per unit of movement velocity remains unchanged.



467

468 **Figure 5.** Bar plots showing the distribution of electromyography (EMG) data for the main dependent
 469 variables that showed significant Day by Condition interaction effects: (A) Reciprocal EMG (B) Co-
 470 Contraction. For both variables, post-hoc t-tests revealed a significant difference across days only for the
 471 SEQ condition and a significant difference between the Sequence (SEQ) and Random (RND) conditions
 472 only on Day 6. (* $p < 0.05$; ** $p < 0.005$). Error bars represent 95% Confidence Interval
 473

474 **DISCUSSION**

475 Here, we investigated the neural correlates mediating the early (fast) and late (slow) motor sequence
 476 learning through the simultaneous acquisition of fMRI data in the brain and cervical spinal cord. Analyses
 477 of the behavioral data revealed that subjects learned the new sequence of movements as they showed
 478 improvements in performance within and between training sessions, hence reflecting both short- and
 479 long-term motor learning, respectively. The between-sessions behavioral changes were also paralleled by
 480 similar changes in EMG metrics, with reduced co-contractions and increased reciprocal EMG activity

481 during sequential movements from the early- to the late-learning phases. Importantly, fMRI results at the
482 spinal cord and brain levels revealed both intra- and inter-sessions learning-related changes in neural
483 activity. As predicted, early learning related activations in the spinal cord were present in a small area
484 located caudally in the C8 segment, ipsilateral to the hand executing the task. By contrast, performance of
485 the learned sequence in the late-learning session was accompanied by widespread and more rostral
486 activations in 3 clusters across C6 and C7 spinal segments. Parallely, increased cerebral activity was
487 observed in inferior frontal and temporal regions as well as in the insula, caudate and cerebellum (Crus I)
488 within the early learning phase, while cerebellar activations in lobules IV and V as well as in the anterior
489 cingulate cortex, cuneus and amygdala were observed in the late-learning session. Between-sessions
490 contrasts revealed increased activations in early vs. late learning in the superior and medial frontal
491 regions, precuneus, inferior parietal, as well as left caudate nucleus. Yet as expected, the opposite contrast
492 (late vs. early) yielded learning-related increased activations in the right putamen, the right posterior
493 cingulate, the right occipital pole, and the right cerebellum lobule IX and vermis lobule VIII. Finally, the
494 connectivity analysis showed that in earlier stages of learning (Day 1), activity in the right cerebellum,
495 left precuneus, and left precentral increased their functional connectivity with the spinal cord ROI (C8).
496 By contrast, during the later stage of learning (Day 6), the increased connectivity with the late-learning
497 related spinal ROI (C6) was observed in the angular gyrus and cerebellum.

498 *Behavioral findings*

499 Consistent with the literature using variants of Serial Reaction Time tasks (SRTT, (13, 40), our behavioral
500 results demonstrate that participants' performance improved both within- as well as across training
501 sessions. This suggests that such improvement was due to learning of the pattern of sequential
502 movements, above and beyond the mere general effect of practicing movements needed to reach targets
503 with a joystick. Across sessions, we also observed further improvements that were specific to the SEQ
504 condition only, hence showing evidence that participants also reached the late MSL phase. In our joystick
505 reaching task, both RND and SEQ performances became faster from Day1 to Day 6 practice, however,
506 the most significant change was manifested in the kinematics data, as calculated by IAJ scores, which
507 evaluates how smoothly the trajectories were performed. Thus in this task, long-term changes in
508 performance due to learning appeared to be better characterized using kinematic measures, rather than
509 through the subjects' performance speed.

510 *Electromyographic findings*

511 The changes in EMG measurements, which paralleled those seen in the behavioral output, are likely to
512 reflect plasticity in the corticospinal circuits and within the spinal cord. This assertion is based on results
513 from a previous electrophysiological study by our group (13), in which we used the same joystick-based

514 SRTT task and H-reflex measurements (assessing activity in the spinal circuitry) acquired pre-, during
515 and post-learning of a new sequence of finger movements. In the latter study, the H-reflex amplitude
516 decreased significantly more in the SEQ, compared with the RND condition, until subjects reached
517 asymptotic performance (i.e., a plateau), indicating that this was related to the sequential content of the
518 task, and not simply a consequence of executing wrist movements. Given that we employed the same task
519 in the current study, it is appropriate to assume that the reduced co-contractions and increased reciprocal
520 EMG activity, are indicators of changes of activity in the spinal and corticospinal circuits as well. Indeed,
521 previous electrophysiology studies that assessed the corticospinal excitability through H-reflex
522 conditioned by transcranial magnetic stimulation over the primary motor cortex (M1), during and after
523 motor skill acquisition, have reported increases in corticospinal excitability (41). Studies that have
524 assessed only the local spinal changes through H-reflexes of muscles involved in executing a motor skill
525 to be learned also found decreases in unconditioned reflex amplitude immediately after learning, both in
526 the upper (42, 43), as well as the lower limbs (44). Interestingly, and in line with the long-term changes in
527 EMG in our study, the decreases in unconditioned H-reflex amplitude reported elsewhere were found to
528 be persistent 24 hours after learning (42). Finally, studies that used conditioned H-reflexes have found
529 reduced homosynaptic H-reflex depression (45) and increased presynaptic inhibition (43), both findings
530 providing evidence for local spinal cord plasticity following motor skill learning. Altogether these
531 findings, and those reported here, suggest that the spinal cord plays a role in the stabilization and
532 facilitation of movement execution, which is achieved through modification of muscle and joint stiffness
533 as the motor skill is being practiced.

534 *Cerebral correlates of short- and long-term motor sequence learning*

535 There is a large body of evidence that MSL is associated with different brain activation patterns following
536 short- and long-term practice (3-5, 7, 46-48). We found a decrease of BOLD activity in the caudate, but
537 an increase of activity in the right putamen from the early to the late learning session; a pattern that has
538 been described in a previous meta-analysis of brain activations associated with long-term motor learning
539 paradigms (4) as well in numerous studies from our laboratory (2, 5, 6). Short- vs. long-term learning has
540 also been associated with an increase of activity in the precuneus, which is thought to be involved in the
541 integration of visuospatial information when attention is required for completing a cue-based task (49),
542 the superior parietal lobule, known to be involved in the spatial integration and motor learning (50), and
543 lateral occipital cortex which is linked to the observation of targets when learning assessed through the
544 use of a SRTT paradigm is required (51). These findings are in accordance with the model of motor skill
545 acquisition which proposes a ‘specialization’ of cortico-striatal and cortico-cerebellar networks as a
546 function of the type of motor skill acquired (5). Yet, contrary to findings of some previous studies (4), we

547 observed an increase in activity in the cerebellum when comparing late vs. early learning sessions.
548 Although conjectural, this apparent discrepancy can be explained by the fact that movements needed to
549 control the joystick have a strong motor adaptation component, in addition to the sequential aspect of the
550 task. The cerebellum is known for its involvement in motor coordination and our previous study has also
551 suggested increased connectivity between the spinal cord and the cerebellum (16). Likewise, our results
552 show an increase in hippocampal activity in late vs. early learning sessions, in apparent contrast with the
553 view proposing that this structure is thought to be particularly implicated in the early, rather than late
554 phase of MSL (47). We believe, however, that this inconsistency may be due again to the spatial nature of
555 the task, which is expected to elicit this structure.

556 *Spinal correlates of short- and long-term motor sequence learning*

557 A plethora of studies have reported evidence of learning-dependent plasticity in the spinal cord following
558 the acquisition of new motor skills (10). Most of these studies employed electrophysiological techniques
559 (e.g., H-reflex) to show changes following the practice of simple motor control tasks or motor learning
560 paradigms (13, 52, 53). Previously, we have provided evidence of the spinal cord's independent
561 contribution to MSL using fMRI and a finger tapping task (16). Despite differences in the task used for
562 measuring MSL, our current results replicate the findings in our previous study, as we show that short-
563 term motor sequence learning measured using a target-reaching task is associated with an increase of
564 activity in the C8 segment of the spinal cord, an area very similar to the one that was activated during the
565 finger MSL task and one that is known to be involved in the control of fine finger and hand movements
566 (16).

567 More importantly, however, in addition to replicating our previous results, the current findings
568 expand them in two critical ways. First, thanks to the spatial resolution achieved with our fMRI pulse
569 sequence, we were now able to determine the lateralization of the activity (ipsilateral to the hand used for
570 the task), and to demonstrate that the peak of activation was in the ventral horn of the spinal cord, where
571 motoneuron cell bodies are located. Additional activation at the center and contralateral side relative to
572 the hand may suggest activation of local spinal interneurons at the commissural level (54). Future studies
573 with higher resolutions can help us to delineate this observation. Second, the present pattern of results
574 shows that similar to the brain, the activation pattern reflecting long-term motor learning in the (C5/C6)
575 spinal cord is distinguishable from that of the short-term motor learning (C7/C8). The C5-C8 spinal
576 segments correspond to myotomes related to the innervation of upper limb muscles (55). Interestingly, the
577 EMG data suggest a decrease in co-contractions between FCR and ECR muscles. This is thus
578 concomitant with the increase in the fine motor control exerted by the wrist flexors and extensors as
579 learning progresses across multiple sessions. The C5-6 is a known hub for most ECR/FCR motoneurons

580 while C7-8 mostly innervates extrinsic finger muscles. A more rostral activation associated with long-
581 term learning is in line with studies suggesting that in motor learning paired with visual feedback, the
582 motor commands involves ECR/FCR muscles during wrist flexion and extension than other muscles like
583 those involving the fingers (56-58). Accordingly, these changes suggest that with more practice,
584 participants develop a more refined motor control by changing the synergy between muscles of the hand
585 and wrist. The optimal feedback theory assumes the existence of redundant anatomical (muscles and
586 joints), kinematic (velocity and trajectory of movement) and neurophysiological (multiple motoneurons
587 innervating different fibers in the same muscle and motoneurons of different muscles receiving common
588 inputs) alternatives to complete a specific action (59, 60). Accordingly, the completion of the same series
589 of actions in a task can be done by changing the synergy between different groups of muscles that could
590 differ substantially from one to another, but still, achieve the task requirements (61). The effects of long-
591 term practice of the motor sequence may have helped the system to elicit the most cost-effective
592 activation pattern of the hand and wrist muscles, combined. The changes in activation from caudal to
593 more rostral segments might thus be related to progressive changes of muscle synergies during learning,
594 with more focal and fine motor control of wrist muscles (motoneurons located at C5-C6 segmental levels)
595 with practice, involving spinal interneurons (spinal cord intermediate zone), and less co-activation of
596 hand muscles (motoneurons located at C7-C8).

597 *Brain-spinal cord interaction in early and late motor sequence learning*

598 Another main contribution of the current study was the assessment of brain-spinal cord interaction during
599 early and late MSL, made possible by the simultaneous fMRI of the brain and cervical spinal cord. The
600 brain regions that were synchronized with those of the spinal cord involved during short-term learning
601 (C8) were the precuneus, thought to be involved in the visuospatial coordination of motor action (62), and
602 the motor cortex in the contralateral hemisphere, as early in the learning of a motor skill the motor cortex
603 is actively involved in the control of every single motor units at the execution site (63). By the end of the
604 learning on Day 1, synchronization between the spinal cord, the motor cortex and the precuneus was no
605 longer significant, and was replaced by an increase in synchronization of activity in the spinal cord and
606 the angular gyrus, a region known to be involved in spatial attention (64). On Day 6, however, we then
607 observed an increase in the synchronization between the spinal cord and angular gyrus, which may
608 suggest that after 5 sessions of practice, attentional mechanisms become more important for the
609 completion of a motor sequence, while for the random practice, we did not see much change on Day 6.
610 Finally, at the end of day 6, activity in the spinal cord and the cerebellum became more synchronized
611 suggestive of a better performance in the SEQ condition, which is a rhythmic practice, synchronization
612 between the cerebellum and the spinal cord is also required (65).

613 Research on the brain-spinal cord interaction in the acquisition of motor skills is mostly driven by
614 studies in animal models. Those studies suggest the existence of differential connections between the
615 interneurons located in the posterior and anterior horn of the spinal cord and the sensory and motor
616 cortices (17). Using a combination of optogenetics, electrophysiology and behavioral assessments in
617 primates, it has been shown that this organization and the interaction between the two subsystems is
618 crucial for skilled motor behaviour: blocking the activity of neurons in the motor cortex and a subgroup of
619 spinal interneurons resulting in impaired movement reaching, while damage to the sensory cortex and
620 another subset of spinal interneurons impaired the release of movements in a goal-oriented task (19). The
621 only previous study which used fMRI to investigate motor learning and the interaction between the brain
622 and spinal cord has supported the idea behind the unique contribution of the human spinal cord to motor
623 learning (16). Yet it should be noted that our previous study focused only on the early stage of the
624 learning and showed similar pattern of connectivity increase between the spinal cord and cerebellum as
625 observed on Day 1 of the current study. In current study, we provide behavioral, electrophysiological and
626 neuroimaging evidence for the long-term spinal cord plasticity related to motor skill acquisition in
627 humans. However, given the organisation of the central nervous system and the anatomical hierarchy
628 between the brain and cord, it would be important to study the causal relationship between these
629 structures during different phases of learning. The PPI analysis does not examine effective connectivity
630 (one approach that allows the statistical estimation of causality) between the brain and the spinal cord.
631 Other methods for estimating effective connectivity in fMRI data might be helpful in deciphering the
632 pattern of causal relationship between the brain and spinal cord signals.

633 Furthermore, there are a few limitations in the current study that need to be considered when designing
634 future studies. Similar to most of neuroimaging studies of motor learning, our sample consists of only
635 right-handed participants, and thus this may have an impact on the lateralisation observed in our results.
636 In addition, because of the nature of block-design GLM analysis on whole spinal cord data, a
637 segmentation of the gray matter was not employed in the current analysis. Besides, we were only able to
638 record EMG from two groups of muscles. Future studies that include more recorded muscle activity or
639 use high-density EMG recording might give better understanding of changes in muscles synergies and
640 their relation to spinal cord activities from early to late motor learning.

641

642 **CONCLUSION**

643 To our knowledge, this study is the first to use fMRI to investigate the spinal cord plasticity and its
644 interaction with the brain associated with short- and long-term learning of a novel motor skill. We
645 demonstrate that, long-term motor learning in the human spinal cord is distinguishable from short-term

646 motor learning, and that the changes in the spinal cord interaction with the brain is related to the
647 requirements of the task at-hand as revealed by the behavioral indicators of motor learning (jerkiness of
648 movements). In a joystick task that relied on the integration of information from visual and motor
649 networks, the increases in movement fluency associated specifically with the long-term acquisition of the
650 motor sequence were associated, not only with specific changes within the spinal cord activity from
651 caudal to rostral segments, but also with a shift in its cerebral connectivity from the sensorimotor network
652 initially, to the attentional network and other brain areas involved in the control of rhythmic motor
653 actions.

654

655 **ACKNOWLEDGMENTS**

656 We would like to thank Mr Benoit Beranger for his help in the preprocessing of EMG data acquired
657 inside the scanner. We also would like to thank Mr Arnaud Boré for his help at different stages of this
658 work and Mr Chadi Sayour for his contribution at data collection stage of the project.

659

660

661
662

References

- 663 1. E. Dayan, L. G. Cohen, Neuroplasticity subserving motor skill learning. *Neuron* **72**, 443-
664 454 (2011).
- 665 2. J. Doyon, H. Benali, Reorganization and plasticity in the adult brain during learning of
666 motor skills. *Curr Opin Neurobiol* **15**, 161-167 (2005).
- 667 3. J. Doyon, E. Gabbitov, S. Vahdat, O. Lungu, A. Boutin, Current issues related to motor
668 sequence learning in humans. *Curr Opin Behav Sci* **20**, 89-97 (2018).
- 669 4. K. R. Lohse, K. Wadden, L. A. Boyd, N. J. Hodges, Motor skill acquisition across short
670 and long time scales: a meta-analysis of neuroimaging data. *Neuropsychologia* **59**, 130-
671 141 (2014).
- 672 5. J. Doyon *et al.*, Contributions of the basal ganglia and functionally related brain
673 structures to motor learning. *Behav Brain Res* **199**, 61-75 (2009).
- 674 6. J. Doyon, V. Penhune, L. G. Ungerleider, Distinct contribution of the cortico-striatal and
675 cortico-cerebellar systems to motor skill learning. *Neuropsychologia* **41**, 252-262 (2003).
- 676 7. S. Lehericy *et al.*, Distinct basal ganglia territories are engaged in early and advanced
677 motor sequence learning. *Proc Natl Acad Sci U S A* **102**, 12566-12571 (2005).
- 678 8. E. Bizzi, M. C. Tresch, P. Saltiel, A. d'Avella, New perspectives on spinal motor systems.
679 *Nat Rev Neurosci* **1**, 101-108 (2000).
- 680 9. J. W. Grau, Learning from the spinal cord: How the study of spinal cord plasticity informs
681 our view of learning. *Neurobiology of Learning and Memory* **108**, 155-171 (2014).
- 682 10. J. R. Wolpaw, Spinal cord plasticity in acquisition and maintenance of motor skills. *Acta*
683 *Physiol (Oxf)* **189**, 155-169 (2007).
- 684 11. P. L. Albuquerque *et al.*, Effects of repetitive transcranial magnetic stimulation and trans-
685 spinal direct current stimulation associated with treadmill exercise in spinal cord and
686 cortical excitability of healthy subjects: A triple-blind, randomized and sham-controlled
687 study. *PLoS One* **13**, e0195276 (2018).
- 688 12. S. Meunier *et al.*, Spinal use-dependent plasticity of synaptic transmission in humans
689 after a single cycling session. *J Physiol* **579**, 375-388 (2007).
- 690 13. O. Lungu *et al.*, Changes in spinal reflex excitability associated with motor sequence
691 learning. *J Neurophysiol* **103**, 2675-2683 (2010).
- 692 14. N. Roche, B. Bussel, M. A. Maier, R. Katz, P. Lindberg, Impact of precision grip tasks on
693 cervical spinal network excitability in humans. *J Physiol* **589**, 3545-3558 (2011).
- 694 15. L. Christiansen, J. Lundbye-Jensen, M. A. Perez, J. B. Nielsen, How plastic are human
695 spinal cord motor circuitries? *Exp Brain Res* **235**, 3243-3249 (2017).
- 696 16. S. Vahdat *et al.*, Simultaneous Brain-Cervical Cord fMRI Reveals Intrinsic Spinal Cord
697 Plasticity during Motor Sequence Learning. *PLoS Biol* **13**, e1002186 (2015).
- 698 17. A. J. Levine, K. A. Lewallen, S. L. Pfaff, Spatial organization of cortical and spinal
699 neurons controlling motor behavior. *Curr Opin Neurobiol* **22**, 812-821 (2012).
- 700 18. A. J. Peters, J. Lee, N. G. Hedrick, K. O'Neil, T. Komiyama, Reorganization of
701 corticospinal output during motor learning. *Nat Neurosci* **20**, 1133-1141 (2017).
- 702 19. M. Ueno *et al.*, Corticospinal Circuits from the Sensory and Motor Cortices Differentially
703 Regulate Skilled Movements through Distinct Spinal Interneurons. *Cell Rep* **23**, 1286-
704 1300 e1287 (2018).
- 705 20. R. G. Mynark, D. M. Koceja, Comparison of soleus H-reflex gain from prone to standing
706 in dancers and controls. *Electroencephalogr Clin Neurophysiol* **105**, 135-140 (1997).
- 707 21. J. Nielsen, C. Crone, H. Hultborn, H-reflexes are smaller in dancers from The Royal
708 Danish Ballet than in well-trained athletes. *European journal of applied physiology and*
709 *occupational physiology* **66**, 116-121 (1993).

- 710 22. R. Ryder, K. Kitano, D. M. Koceja, Spinal reflex adaptation in dancers changes with
711 body orientation and role of pre-synaptic inhibition. *Journal of dance medicine & science*
712 : official publication of the International Association for Dance Medicine & Science **14**,
713 155-162 (2010).
- 714 23. W. Taube *et al.*, Differential reflex adaptations following sensorimotor and strength
715 training in young elite athletes. *International journal of sports medicine* **28**, 999-1005
716 (2007).
- 717 24. D. R. Earles, J. T. Dierking, C. T. Robertson, D. M. Koceja, Pre- and post-synaptic
718 control of motoneuron excitability in athletes. *Medicine and science in sports and*
719 *exercise* **34**, 1766-1772 (2002).
- 720 25. V. Monda *et al.*, Primary Motor Cortex Excitability in Karate Athletes: A Transcranial
721 Magnetic Stimulation Study. *Front Physiol* **8**, 695 (2017).
- 722 26. F. Moscatelli *et al.*, Functional Assessment of Corticospinal System Excitability in Karate
723 Athletes. *PLoS One* **11**, e0155998 (2016).
- 724 27. F. Moscatelli *et al.*, Differences in corticospinal system activity and reaction response
725 between karate athletes and non-athletes. *Neurol Sci* **37**, 1947-1953 (2016).
- 726 28. J. Cohen-Adad *et al.*, BOLD signal responses to controlled hypercapnia in human spinal
727 cord. *Neuroimage* **50**, 1074-1084 (2010).
- 728 29. J. Finsterbusch, C. Sprenger, C. Buchel, Combined T2*-weighted measurements of the
729 human brain and cervical spinal cord with a dynamic shim update. *Neuroimage* **79**, 153-
730 161 (2013).
- 731 30. S. Vahdat *et al.*, Resting-state brain and spinal cord networks in humans are functionally
732 integrated. *PLoS Biol* **18**, e3000789 (2020).
- 733 31. A. Tinnermann, S. Geuter, C. Sprenger, J. Finsterbusch, C. Buchel, Interactions
734 between brain and spinal cord mediate value effects in nocebo hyperalgesia. *Science*
735 **358**, 105-108 (2017).
- 736 32. J. Finsterbusch, F. Eippert, C. Buchel, Single, slice-specific z-shim gradient pulses
737 improve T2*-weighted imaging of the spinal cord. *Neuroimage* **59**, 2307-2315 (2012).
- 738 33. B. De Leener *et al.*, SCT: Spinal Cord Toolbox, an open-source software for processing
739 spinal cord MRI data. *Neuroimage* **145**, 24-43 (2017).
- 740 34. M. Jenkinson, C. F. Beckmann, T. E. Behrens, M. W. Woolrich, S. M. Smith, Fsl.
741 *Neuroimage* **62**, 782-790 (2012).
- 742 35. S. Balasubramanian, A. Melendez-Calderon, A. Roby-Brami, E. Burdet, On the analysis
743 of movement smoothness. *J Neuroeng Rehabil* **12**, 112 (2015).
- 744 36. D. Goldvasser, C. A. McGibbon, D. E. Krebs, High curvature and jerk analyses of arm
745 ataxia. *Biol Cybern* **84**, 85-90 (2001).
- 746 37. C. L. Banks, H. J. Huang, V. L. Little, C. Patten, Electromyography Exposes
747 Heterogeneity in Muscle Co-Contraction following Stroke. *Front Neurol* **8** (2017).
- 748 38. M. Flanders, P. J. Cordo, Quantification of Peripherally Induced Reciprocal Activation
749 during Voluntary Muscle-Contraction. *Electroen Clin Neuro* **67**, 389-394 (1987).
- 750 39. A. L. Hof, H. Elzinga, W. Grimmius, J. P. K. Halbertsma, Speed dependence of
751 averaged EMG profiles in walking. *Gait Posture* **16**, 78-86 (2002).
- 752 40. M. J. Nissen, P. Bullemer, Attentional requirements of learning: Evidence from
753 performance measures. *Cognitive Psychology* **19**, 1-32 (1987).
- 754 41. P. Wiegel, C. Leukel, Training of a discrete motor skill in humans is accompanied by
755 increased excitability of the fastest corticospinal connections at movement onset. *J*
756 *Physiol* **598**, 3485-3500 (2020).
- 757 42. L. S. Giboin, C. Tokuno, A. Kramer, M. Henry, M. Gruber, Motor learning induces time-
758 dependent plasticity that is observable at the spinal cord level. *J Physiol* **598**, 1943-1963
759 (2020).

- 760 43. K. Kitano, M. Tsuruike, C. T. Robertson, D. M. Kocejaj, Effects of a complex balance
761 task on soleus H-reflex and presynaptic inhibition in humans. *Electromyogr Clin*
762 *Neurophysiol* **49**, 235-243 (2009).
- 763 44. R. Mazzocchio, T. Kitago, G. Liuzzi, J. R. Wolpaw, L. G. Cohen, Plastic changes in the
764 human H-reflex pathway at rest following skillful cycling training. *Clin Neurophysiol* **117**,
765 1682-1691 (2006).
- 766 45. T. Winkler, B. Mergner, J. Szecsi, A. Bender, A. Straube, Spinal and cortical activity-
767 dependent plasticity following learning of complex arm movements in humans. *Exp Brain*
768 *Res* **219**, 267-274 (2012).
- 769 46. J. Doyon, Neural and physiological substrates mediating motor skill learning and
770 consolidation. *Journal of Sport & Exercise Psychology* **38**, S4-S4 (2016).
- 771 47. G. Albouy, B. R. King, P. Maquet, J. Doyon, Hippocampus and Striatum: Dynamics and
772 Interaction During Acquisition and Sleep-Related Motor Sequence Memory
773 Consolidation. *Hippocampus* **23**, 985-1004 (2013).
- 774 48. L. G. Ungerleider, J. Doyon, A. Karni, Imaging brain plasticity during motor skill learning.
775 *Neurobiol Learn Mem* **78**, 553-564 (2002).
- 776 49. D. Nardo, V. Santangelo, E. Macaluso, Stimulus-driven orienting of visuo-spatial
777 attention in complex dynamic environments. *Neuron* **69**, 1015-1028 (2011).
- 778 50. D. Coynel *et al.*, Dynamics of motor-related functional integration during motor sequence
779 learning. *Neuroimage* **49**, 759-766 (2010).
- 780 51. I. Rothkirch, S. Wolff, N. G. Margraf, A. Pedersen, K. Witt, Does Post-task Declarative
781 Learning Have an Influence on Early Motor Memory Consolidation Over Day? An fMRI
782 Study. *Front Neurosci* **12**, 280 (2018).
- 783 52. M. L. Evatt, S. L. Wolf, R. L. Segal, Modification of human spinal stretch reflexes:
784 preliminary studies. *Neurosci Lett* **105**, 350-355 (1989).
- 785 53. J. S. Carp, A. M. Tennissen, X. Y. Chen, J. R. Wolpaw, H-reflex operant conditioning in
786 mice. *J Neurophysiol* **96**, 1718-1727 (2006).
- 787 54. B. Hanna-Boutros, S. Sangari, A. Karasu, L. S. Giboin, V. Marchand-Pauvert, Task-
788 related modulation of crossed spinal inhibition between human lower limbs. *J*
789 *Neurophysiol* **111**, 1865-1876 (2014).
- 790 55. F. H. Martini, R. B. Tallitsch, J. L. Nath, *Human Anatomy* (Pearson, London, England,
791 ed. 9, 2018).
- 792 56. F. Danion *et al.*, A mode hypothesis for finger interaction during multi-finger force-
793 production tasks. *Biol Cybern* **88**, 91-98 (2003).
- 794 57. S. Ambike, D. Mattos, V. M. Zatsiorsky, M. L. Latash, Unsteady steady-states: central
795 causes of unintentional force drift. *Exp Brain Res* **234**, 3597-3611 (2016).
- 796 58. J. Hirose, C. Cuadra, C. Walter, M. L. Latash, Finger interdependence and unintentional
797 force drifts: Lessons from manipulations of visual feedback. *Hum Mov Sci* **74**, 102714
798 (2020).
- 799 59. E. Pierrot-Deseilligny, D. Burke, *The Circuitry of the Human Spinal Cord: Spinal and*
800 *Corticospinal Mechanisms of Movement* (Cambridge University Press, Cambridge,
801 2012), DOI: 10.1017/CBO9781139026727.
- 802 60. S. H. Scott, Optimal feedback control and the neural basis of volitional motor control. *Nat*
803 *Rev Neurosci* **5**, 532-546 (2004).
- 804 61. M. H. Sohn, J. L. McKay, L. H. Ting, Defining feasible bounds on muscle activation in a
805 redundant biomechanical task: practical implications of redundancy. *J Biomech* **46**,
806 1363-1368 (2013).
- 807 62. N. Wenderoth, F. Debaere, S. Sunaert, S. P. Swinnen, The role of anterior cingulate
808 cortex and precuneus in the coordination of motor behaviour. *Eur J Neurosci* **22**, 235-
809 246 (2005).

- 810 63. N. F. Wymbs, D. S. Bassett, P. J. Mucha, M. A. Porter, S. T. Grafton, Differential
811 recruitment of the sensorimotor putamen and frontoparietal cortex during motor chunking
812 in humans. *Neuron* **74**, 936-946 (2012).
- 813 64. Q. Chen, R. Weidner, S. Vossel, P. H. Weiss, G. R. Fink, Neural mechanisms of
814 attentional reorienting in three-dimensional space. *J Neurosci* **32**, 13352-13362 (2012).
- 815 65. Y. I. Arshavsky, G. N. Orlovsky, "Role of the Cerebellum in the Control of Rhythmic
816 Movements" in *Neurobiology of Vertebrate Locomotion*, G. S., Stein P.S.G., S. D.G., F.
817 H., H. R.M., Eds. (Palgrave Macmillan, London, 1986), pp. 677-689.
- 818
- 819